Acta Crystallographica Section D
Biological Crystallography
ISSN 0907-4449

Anomalous signal from S atoms in protein crystallographic data from an X-ray free-electron laser

Thomas R. M. Barends,[a,b]*‡ Lutz Foucar,[a,b]‡ Robert L. Shoeman,[a,b] Sadia Bari,[b,c] Sascha W. Epp,[b,c] Robert Hartmann,[d] Gunter Hauser,[e,f] Martin Huth,[d,e] Christian Kieser,[a] Lukas Lomb,[a,b] Koji Motomura,[g] Kiyonobu Nagaya,[h,i] Carlo Schmidt,[b,c] Rafael Strecker,[e,f] Denis Anielski,[b,c] Rebecca Boll,[b,c] Benjamin Erk,[b,c] Hironobu Fukuzawa,[g,i] Elisabeth Hartmann,[a] Takaki Hatsui,[i] Peter Holl,[d] Yuichi Inubushi,[i] Tetsuya Ishikawa,[i] Stephan Kassemeyer,[a,b] Christian Kaiser,[c] Frank Koeck,[c] Naoki Kunishima,[i] Moritz Kurka,[c] Daniel Rolles,[a,b] Benedikt Rudek,[b,c] Artem Rudenko,[b,c,j] Takahiro Sato,[i] Claus-Dieter Schroeter,[c] Heike Soltau,[d] Lothar Strueder,[e,k] Tomoyuki Tanaka,[i] Tadashi Togashi,[i] Kensuke Tono,[l] Joachim Ullrich,[b,c] Satoshi Yase,[h] Shin-ichi Wada,[i,m] Makoto Yao,[h] Makina Yabashi,[i] Kiyoshi Ueda[g,i] and Ilme Schlichting[a,b]*

[a]Max-Planck-Institut für medizinische Forschung, Jahnstrasse 29, 69120 Heidelberg, Germany, [b]Max Planck Advanced Study Group, Center for Free-Electron Laser Science (CFEL), Notkestrasse 85, 22607 Hamburg, Germany, [c]Max-Planck-Institut für Kernphysik, Saupfercheckweg 1, 69117 Heidelberg, Germany, [d]PNSensor GmbH, Otto-Hahn-Ring 6, 81739 München, Germany, [e]Max-Planck-Institut Halbleiterlabor, Otto-Hahn-Ring 6, 81739 München, Germany, [f]Max-Planck-Institut für extraterrestrische Physik, Giessenbachstrasse, 85741 Garching, Germany, [g]Institute of Multi-disciplinary Research for Advanced Materials, Tohoku University, Sendai 980-8577, Japan, [h]Department of Physics, Kyoto University, Kyoto 606-8502, Japan, [i]RIKEN SPring-8 Center, Kouto 1-1-1, Sayo, Hyogo 679-5148, Japan, [j]J. R. Macdonald Laboratory, Department of Physics, Kansas State University, Manhattan, KS 66506, USA, [k]University of Siegen, Emmy-Noether Campus, Walter Flex Strasse, 57068 Siegen, Germany, [l]Japan Synchrotron Radiation Research Institute (JASRI), Kouto 1-1-1, Sayo, Hyogo 679-5198, Japan, and [m]Department of Physical Science, Hiroshima University, Higashi-Hiroshima 739-8526, Japan

‡ These authors contributed equally.

Correspondence e-mail: thomas.barends@mpimf-heidelberg.mpg.de, ilme.schlichting@mpimf-heidelberg.mpg.de

Received 31 October 2012
Accepted 24 January 2013

X-ray free-electron lasers (FELs) enable crystallographic data collection using extremely bright femtosecond pulses from microscopic crystals beyond the limitations of conventional radiation damage. This diffraction-before-destruction approach requires a new crystal for each FEL shot and, since the crystals cannot be rotated during the X-ray pulse, data collection requires averaging over many different crystals and a Monte Carlo integration of the diffraction intensities, making the accurate determination of structure factors challenging. To investigate whether sufficient accuracy can be attained for the measurement of anomalous signal, a large data set was collected from lysozyme microcrystals at the newly established 'multi-purpose spectroscopy/imaging instrument' of the SPring-8 Ångstrom Compact Free-Electron Laser (SACLA) at RIKEN Harima. Anomalous difference density maps calculated from these data demonstrate that serial femtosecond crystallography using a free-electron laser is sufficiently accurate to measure even the very weak anomalous signal of naturally occurring S atoms in a protein at a photon energy of 7.3 keV.

1. Introduction

X-ray free-electron lasers (FELs) provide extremely intense femtosecond pulses that promise the high-resolution structure determination of tiny crystals by 'outrunning' radiation damage. Because FELs reduce the requirements on crystal size, they are of immediate relevance for the study of the large group of difficult-to-crystallize molecules that yield only small crystals. Therefore, crystallographic data collection from protein crystals using free-electron laser sources has recently seen a surge in interest. After the initial proof-of-principle experiments described by Chapman *et al.* (2011), a number of reports have been published showing the feasibility of studying small crystals grown *in vivo* (Koopmann *et al.*, 2012) or in the sponge phase (Johansson *et al.*, 2012) and of performing time-resolved pump-probe experiments (Aquila *et al.*, 2012; Kern *et al.*, 2012) as well as demonstrating that FELs enable high-resolution structural analysis by using a well established model system (Boutet *et al.*, 2012). These studies relied on progress in working out the particular challenges associated with serial femtosecond crystallography (SFX) data collection using FEL light sources (Kirian *et al.*, 2010, 2011; White *et al.*, 2012) and the implementation of the *CrystFEL* software suite for SFX data processing (White *et al.*, 2012).

In SFX, randomly oriented crystals are introduced into the FEL beam in a small liquid jet in their mother liquor at room temperature. The many diffraction snapshots required for a complete three-dimensional diffraction data set are acquired

in a serial fashion, since the crystals are destroyed by the FEL pulses within femtoseconds after providing a useful diffraction pattern (Neutze *et al.*, 2000; Barty *et al.*, 2012; Caleman, Bergh *et al.*, 2011; Caleman, Huldt *et al.*, 2011; Lomb *et al.*, 2011). Consequently, any data-processing algorithm has to account for variations in crystal size and quality. Moreover, FEL fluences and spectra usually vary widely from shot to shot, causing further variation in the measured data. Apart from this, on the timescale of a femtosecond FEL pulse the crystals cannot be rotated during exposure, causing all data frames to be still images. This, together with the relatively small bandwidth of FEL beams (0.5% in the current study), causes all Bragg spots to be partially rather than fully recorded reflections, *i.e.* thin slices through reciprocal-space lattice nodes.

To obtain integrated Bragg intensities, SFX has so far relied on Monte Carlo integration of diffraction intensities (Kirian *et al.*, 2011; White *et al.*, 2012), in which a large number of images are separately indexed and integrated, after which the intensities are averaged. Provided that a sufficiently large number of observations are made and that crystal orientation space is sufficiently sampled, this results in completely integrated Bragg intensities and averages out the variations in crystal size and quality and in beam properties (Kirian *et al.*, 2010, 2011; White *et al.*, 2012).

While this method has been very successful, phasing serial femtosecond crystallographic data has so far relied on molecular replacement (Boutet *et al.*, 2012; Chapman *et al.*, 2011; Johansson *et al.*, 2012; Redecke *et al.*, 2013). Although other, FEL-specific, phasing methods have been proposed (Son *et al.*, 2011; Spence *et al.*, 2011), classical *de novo* structure determination would require a phasing method such as MIR, SAD or MAD, which crucially depend on highly accurate measurements. To date, it has not yet been shown that the weak intensity differences on which these methods rely can indeed be measured using serial femtosecond crystallography.

An additional complication arises in certain cases where the rotational symmetry of the lattice is higher than that of the space group (such as for the polar space groups, *i.e.* $P3_x$, $P4_x$, $P6_x$ *etc.*). In these cases, an indexing ambiguity exists which has to be resolved before merging data from any two crystals. It is important to realise that this may occur either because of the inherent symmetry of the lattice or because of 'accidental' (pseudo)symmetry caused by the lattice metric, *e.g.* a monoclinic lattice with $\beta \simeq 90^\circ$ or an orthorhombic lattice with $a \simeq b$. Whereas in conventional crystallography the correct choice of indexing is easily determined by comparing the two data sets, for SFX this problem has not yet been solved, as only very few of the diffraction patterns will contain sufficient common reflections for a common indexing to be easily established, and in any event all of these reflections are only partially recorded. Thus, this has so far been neglected in SFX experiments and whenever this problem occurred the data were treated as being perfectly merohedrally twinned (Chapman *et al.*, 2011; White *et al.*, 2012). However, for many protein crystals this complication does not occur. Moreover, since this ambiguity arises from rotational symmetry, not from mirror symmetry, it does not in principle cancel out anomalous differences, although in practice it may be expected to greatly complicate their analysis.

To explore whether SFX data may in principle be used for classical phasing, we collected a highly redundant SFX data set for tetragonal lysozyme (which crystallizes in the nonpolar space group $P4_32_12$, *i.e.* no indexing ambiguity exists) as part of the commissioning of the multi-purpose spectroscopy/imaging apparatus for in-vacuum-type experiments at the SPring-8 Ångstrom Compact Free-Electron Laser (SACLA) at RIKEN Harima in Japan (Ishikawa *et al.*, 2012) and looked for anomalous differences arising from the endogenous sulfur in the protein. Since at the photon energy used (7.3 keV) the tabulated f'' of sulfur is only 0.7 e^-, the anomalous signal is expected to be very weak and therefore represents a perfect test case for the accuracy that may be attained by Monte Carlo integration of SFX intensities.

2. Materials and methods

2.1. Crystal preparation and injection

Hen egg-white lysozyme (Sigma–Aldrich, Schnelldorf, Germany) was crystallized essentially as described previously (Boutet *et al.*, 2012). The microcrystalline suspension was filtered through a 2 µm stainless-steel filter and kept at 293 K in a rotary antisettling device as described previously (Lomb *et al.*, 2012) during data collection. The microcrystals were injected with an HPLC system (Shimadzu Biotech, Duisburg, Germany) into the vacuum chamber in an ∼5 µm wide liquid jet produced with a gas dynamic virtual nozzle (DePonte *et al.*, 2008; Shapiro *et al.*, 2008) housed in a liquid injector (Weierstall *et al.*, 2012) as described previously (Boutet *et al.*, 2012; Chapman *et al.*, 2011). In general, the sample flow rate was 15–20 µl min^{-1}.

2.2. Data collection

The SFX experiment was performed during commissioning time in the multi-purpose spectroscopy/imaging apparatus built by the Tohoku–Kyoto group for in-vacuum-type experiments, which was modelled on the CAMP instrument (Strüder *et al.*, 2010) and housed in Experimental Hutch 3 of BL-3 (Ishikawa *et al.*, 2012). A two-panel pnCCD detector comprising 1024 × 1024 pixels (Strüder *et al.*, 2010) was placed ∼66 mm downstream of the interaction region (limiting the resolution to 3.2 Å at the edge of the detector) and used for diffraction data collection in 14-bit imaging mode for single-shot diffraction data. Microcrystals of HEWL were exposed to single 7.3 keV (1.7 Å, with a bandwidth of 0.5%) X-ray pulses of (nominally) 10 fs duration focused to 1 μm^2 at the interaction point using Kirkpatrick–Baez mirrors. The average photon pulse energy was 0.1 mJ, and was 0.06 mJ at the sample taking into account a beamline transmission of 60%. Single-shot pnCCD frames were recorded at 10 Hz, the repetition rate of the FEL, while the liquid jet was flowing. All detector frames were saved, regardless of whether a given shot contained a hit crystal. Hits were identified online using *CASS* (Foucar *et al.*, 2012). The hit rate was plotted and used to

manually optimize the jet position. A data rate of 20 MB s^{-1} was sustained for the duration of the experiment. Detailed analysis of detector images was performed offline with *CASS* (Foucar *et al.*, 2012). To identify possible hits, only regions of the detector that did not show signal originating from the water jet were considered. After applying a mask, those frames which contained at least one possible Bragg peak were regarded as possible crystal hits. These selected frames were then written out for further processing.

2.3. Data processing

To calibrate the detector geometry, images containing diffraction patterns were summed to obtain a virtual powder pattern. The Debye–Scherrer rings in this pattern were used to determine the position of the direct beam and the distance for each of the two independent pnCCD panels. The Zaefferer algorithm as implemented in *CrystFEL* (White *et al.*, 2012) was then used to identify peaks in the diffraction images, which were then passed on to *DIRAX* (Duisenberg, 1992) and *MOSFLM* (Leslie, 2006; Powell, 1999) for indexing. Peaks that could be indexed using the unit-cell parameters of tetragonal lysozyme were integrated by *CrystFEL*. After integration, the intensities were merged assuming 422 point-group symmetry. The *CrystFEL* intensities were then converted to structure-factor amplitudes and anomalous differences using *XDSCONV* (Kabsch, 1993, 2010*a*,*b*).

3. Results and discussion

Using *CASS*, 420 924 potential hits were identified from 584 274 detector frames. Of these diffraction patterns, 43 840 could be indexed using the expected unit cell. Monte Carlo integration yielded a 3.2 Å resolution data set in which each reflection had been at least partially observed more than 1100 times (>7500 times on average), yielding an $R_{\rm split}$ (White *et al.*, 2012) of 6.9% (see Table 1).

To observe the anomalous signal of the S atoms inherently present in the protein, an anomalous difference density map was calculated with *CCP*4 (Winn *et al.*, 2011) using lysozyme phases obtained by molecular replacement, which showed clear difference density associated with S atoms in the lysozyme structure.

In the anomalous difference density map calculated with data to 3.5 Å resolution, the highest peak (4.5σ) was associated with the Met105 S atom (Fig. 1*a*). Other anomalous difference density peaks (>2.5σ) were found at the positions of the disulfide bonds Cys6–Cys127, Cys64–Cys80 and Cys76–Cys94 (Fig. 1*b*). The other S atoms, *i.e.* the Cys30–Cys115 disulfide bond as well as the Met12 S^{δ} atom, were not associated with anomalous difference density. Moreover, several density peaks not associated with S atoms are present. Since several of these peaks are found on the protein surface, at least some of them might be caused by chloride ions or other anomalous scatterers from the solvent, which contained 10% NaCl and 1 *M* sodium acetate. Indeed, a 3.4σ peak corresponds to the position of a chloride ion observed in the lysozyme structure deposited as PDB entry 3tmu (Kmetko *et al.*, 2011) and another 3.3σ peak corresponds to the position of a rhenium ion in PDB entry 3a93 (Ueno *et al.*, 2010). However, many other peaks may simply arise from the high noise level in the map.

Table 1
Data statistics.

Space group	$P4_32_12$
Unit-cell parameters (Å, °)	$a = b = 77.2$, $c = 37.4$, $\alpha = \beta = \gamma = 90$
Resolution (Å)	56–3.2
No. of diffraction images	420924
No. of indexed patterns	43840
Indexing fraction (%)	10.4
No. of unique reflections	2200
Completeness (%)	100

$R_{\rm split}$† in resolution bins.

$D_{\rm min}$ (Å)	$D_{\rm max}$ (Å)	$R_{\rm split}$ (%)
55.86	8.68	4.21
8.68	6.89	6.08
6.89	6.02	6.53
6.02	5.47	7.44
5.47	5.08	6.03
5.08	4.78	7.33
4.78	4.54	7.09
4.54	4.34	5.93
4.34	4.18	6.94
4.18	4.03	6.84
4.03	3.91	7.21
3.91	3.79	6.59
3.79	3.69	6.80
3.69	3.60	7.40
3.60	3.52	7.42
3.52	3.45	7.87
3.45	3.38	8.99
3.38	3.31	8.32
3.31	3.26	10.49
3.26	3.20	8.62

† $R_{\rm split} = (1/2^{1/2})[|I_{\rm odd} - I_{\rm even}|/(\frac{1}{2}|I_{\rm odd} + I_{\rm even}|)]$ (see White *et al.*, 2012).

For comparison, we collected a data set for tetragonal lysozyme with 20-fold redundancy using conventional methods on a rotating anode (Cu $K\alpha$ radiation). Using these data to 3.8 Å resolution, all S atoms are associated with clear density in an anomalous difference Fourier map, with peak heights ranging from 5.3σ for Met105 to 7.6σ for the Cys76–Cys94 disulfide bond. Thus, in terms of anomalous signal the FEL data clearly suffer from a lower signal-to-noise ratio compared with conventional data. At least in part, this may be expected to arise from the inherent shot-to-shot variation in the FEL beam properties. By using a seeded FEL beam (Amann *et al.*, 2012; Yabashi & Tanaka, 2012), as is for example being proposed for upcoming experiments at LCLS, these shot-to-shot variations are expected to be significantly reduced, which may lead to a substantial improvement in SFX data quality.

It has been hypothesized that electron-rich sites inside a protein, such as S atoms, might be 'hotspots' for specific radiation damage caused by the intense FEL beam (Lomb *et al.*, 2011). In the experiment described here, ~10 fs pulses were used containing $\sim 5 \times 10^{10}$ photons each, resulting in an

average dose of ∼64 MGy per crystal, which is about the dose used in the experiments described in Boutet *et al.* (2012), in which radiation damage was not observed. Given the intermediate resolution (3.2 Å) of the current experiment, the possibility of specific radiation damage cannot be ruled out entirely based on the electron density. However, using the absorption cross-section for sulfur at 7.3 keV of 6.465 × 10^3 barn (NIST; http://physics.nist.gov/PhysRefData/Xcom/html/xcom1.html), on average only 3.3% of all photons impinging on an S atom are absorbed per shot, which should be negligible for our analysis. This is also orders of magnitude below the conditions considered by Hau-Riege *et al.* (2004) under which the use of time-dependent atomic form factors for analysis would be required.

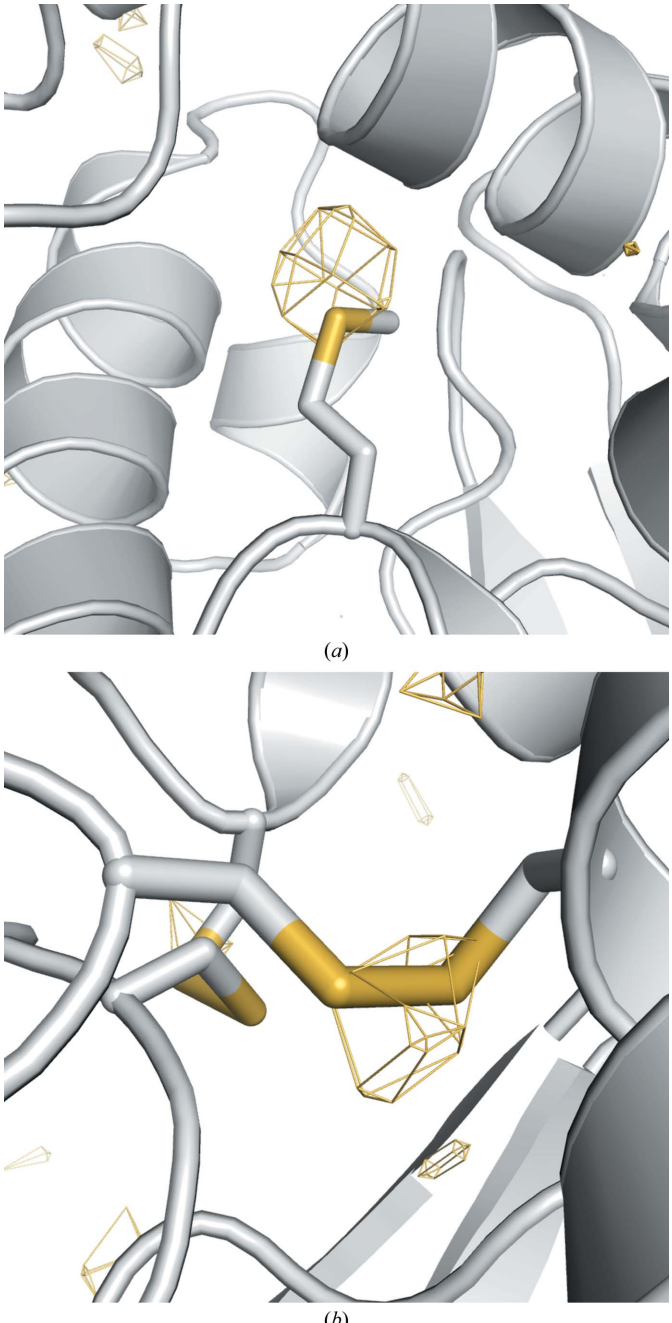

Figure 1
Anomalous difference Fourier maps (yellow) for (*a*) Met105 contoured at 3σ and (*b*) the Cys76–Cys94 disulfide bond contoured at 2.5σ. The molecular-replacement search model (PDB entry 1vds; S. Aibara, A. Suzuki, A. Kidera, K. Shibata, T. L. J. D. Yamane & M. Hirose, unpublished work) is shown in grey.

Attempts at solving the anomalous substructure failed, which is not surprising given the extremely small signal from sulfur at this photon energy and resolution, as can be seen in the noisy nature of the density maps as described above. However, the results presented here clearly demonstrate that despite the obvious challenges associated with the analysis and evaluation of diffraction data collected with free-electron laser sources, anomalous data can be obtained by serial femtosecond crystallography. Thus, serial femtosecond crystallography could potentially be used for *de novo* macromolecular structure determination by SAD, MAD, SIRAS and MIRAS. Moreover, a variation on radiation-damage-induced phasing with anomalous scattering (RIPAS; Zwart *et al.*, 2004; Ramagopal *et al.*, 2005) which depends on the extremely high fluence of FELs has recently been proposed (Son *et al.*, 2011). In this method, the specific removal of inner-shell electrons from heavy atoms by a high-fluence FEL beam results in altered scattering properties when compared with data from a lower-fluence FEL beam. By collecting both high-fluence and low-fluence data these differences may be used for phasing in a manner analogous to the conventional RIPAS method. The data presented here also show that in principle the anomalous component of such data could indeed be collected using serial femtosecond crystallography.

This would open the way to large-scale structure determination efforts of difficult-to-crystallize proteins at the new X-ray FEL sources that are currently in operation (SACLA and LCLS) or are being built (such as SwissFEL and the European XFEL).

4. Supplementary information

An mmCIF file containing structure-factor amplitudes and anomalous differences is available as Supplementary Material[1].

Experiments were carried out at the SPring-8 Ångstrom Compact Free-Electron Laser (SACLA), a national user facility operated by RIKEN. We thank Shimadzu Biotech (Duisburg, Germany) for providing the HPLC system for these experiments. We acknowledge support from the Max Planck Society for funding the ASG at CFEL and from the Ministry of Education, Culture, Sports, Science and Technology of Japan for funding the X-ray Free-Electron Laser Utilization Research Project. We especially thank the staff of the SACLA/RIKEN for their outstanding facility and support in carrying out these experiments. Author contributions are as follows. TRMB, LF, IS, LS, JU and KU conceived the experiment, which was designed with RH, RLS and MYab.

[1] Supplementary material has been deposited in the IUCr electronic archive (Reference: CB5024). Services for accessing this material are described at the back of the journal.

TH, NK, IS, TTa and TI prepared the sample. Sample delivery and injection was performed by SB, LL, CK and RLS. DA, RB, SE, BE, LB, HF, CK, MK, KM, KN, DR, BR, AR, CS, SDS, KU, JU and MYao designed, built and commissioned the Tohoku–Kyoto multi-purpose spectroscopy/imaging apparatus; SFX experiments were carried out by TRMB, SB, SE, LF, HF, RH, GH, MH, CK, LL, KM, KN, IS, CS, RLS, RS, KU, SW, MYab, MYao and SY. The pnCCD detectors were designed, built, set up and operated by RH, GH, PH, MH, HS, RS and LS. The beamline was conceived, designed and operated by TH, YI, KT, TS, TTo and TI. GH, MH, RH, FK, LF, SK, RS and TRMB dealt with and analyzed the diffraction data and TRMB performed the crystallographic analysis. The manuscript was prepared by TRMB, LF and IS, with discussions and improvements from all authors.

References

Amann, J. *et al.* (2012). *Nature Photonics*, **6**, 693–698.
Aquila, A. *et al.* (2012). *Opt. Express*, **20**, 2706–2716.
Barty, A. *et al.* (2012). *Nature Photonics*, **6**, 35–40.
Boutet, S. *et al.* (2012). *Science*, **337**, 362–364.
Caleman, C., Bergh, M., Scott, H. A., Spence, J. C., Chapman, H. N. & Tîmneanu, N. (2011). *J. Mod. Opt.* **58**, 1486–1497.
Caleman, C., Huldt, G., Maia, F. R. N. C., Ortiz, C., Parak, F. G., Hajdu, J., van der Spoel, D., Chapman, H. N. & Timneanu, N. (2011). *ACS Nano*, **5**, 139–146.
Chapman, H. N. *et al.* (2011). *Nature (London)*, **470**, 73–77.
DePonte, D. P., Weierstall, U., Schmidt, K., Warner, J., Starodub, D., Spence, J. C. H. & Doak, R. B. (2008). *J. Phys. D Appl. Phys.* **41**, 195505.
Duisenberg, A. J. M. (1992). *J. Appl. Cryst.* **25**, 92–96.
Foucar, L., Barty, A., Coppola, N., Hartmann, R., Holl, P., Hoppe, U., Kassemeyer, S., Kimmel, N., Küpper, J., Scholz, M., Techert, S., White, T. A., Strüder, L. & Ullrich, J. (2012). *Comput. Phys. Commun.* **183**, 2207–2213.
Hau-Riege, S., London, R. & Szoke, A. (2004). *Phys. Rev. E*, **69**, 051906.
Ishikawa, T. *et al.* (2012). *Nature Photonics*, **6**, 540–544.
Johansson, L. C. *et al.* (2012). *Nature Methods*, **9**, 263–265.
Kabsch, W. (1993). *J. Appl. Cryst.* **26**, 795–800.
Kabsch, W. (2010*a*). *Acta Cryst.* D**66**, 125–132.
Kabsch, W. (2010*b*). *Acta Cryst.* D**66**, 133–144.
Kern, J. *et al.* (2012). *Proc. Natl Acad. Sci. USA*, **109**, 9721–9726.
Kirian, R. A., Wang, X., Weierstall, U., Schmidt, K. E., Spence, J. C., Hunter, M., Fromme, P., White, T., Chapman, H. N. & Holton, J. (2010). *Opt. Express*, **18**, 5713–5723.
Kirian, R. A., White, T. A., Holton, J. M., Chapman, H. N., Fromme, P., Barty, A., Lomb, L., Aquila, A., Maia, F. R. N. C., Martin, A. V., Fromme, R., Wang, X., Hunter, M. S., Schmidt, K. E. & Spence, J. C. H. (2011). *Acta Cryst.* A**67**, 131–140.
Kmetko, J., Warkentin, M., Englich, U. & Thorne, R. E. (2011). *Acta Cryst.* D**67**, 881–893.
Koopmann, R. *et al.* (2012). *Nature Methods*, **9**, 259–262.
Leslie, A. G. W. (2006). *Acta Cryst.* D**62**, 48–57.
Lomb, L. *et al.* (2011). *Phys. Rev. B*, **84**, 214111.
Lomb, L., Steinbrener, J., Bari, S., Beisel, D., Berndt, D., Kieser, C., Lukat, M., Neef, N. & Shoeman, R. L. (2012). *J. Appl. Cryst.* **45**, 674–678.
Neutze, R., Wouts, R., van der Spoel, D., Weckert, E. & Hajdu, J. (2000). *Nature (London)*, **406**, 752–757.
Powell, H. R. (1999). *Acta Cryst.* D**55**, 1690–1695.
Ramagopal, U. A., Dauter, Z., Thirumuruhan, R., Fedorov, E. & Almo, S. C. (2005). *Acta Cryst.* D**61**, 1289–1298.
Redecke, L. *et al.* (2013). *Science*, **339**, 227–230.
Shapiro, D. A., Chapman, H. N., DePonte, D., Doak, R. B., Fromme, P., Hembree, G., Hunter, M., Marchesini, S., Schmidt, K., Spence, J., Starodub, D. & Weierstall, U. (2008). *J. Synchrotron Rad.* **15**, 593–599.
Son, S.-K., Chapman, H. N. & Santra, R. (2011). *Phys. Rev. Lett.* **107**, 218102.
Spence, J. C., Kirian, R. A., Wang, X., Weierstall, U., Schmidt, K. E., White, T., Barty, A., Chapman, H. N., Marchesini, S. & Holton, J. (2011). *Opt. Express*, **19**, 2866–2873.
Strüder, L. *et al.* (2010). *Nucl. Instrum. Methods Phys. Res. A*, **614**, 483–496.
Ueno, T., Abe, S., Koshiyama, T., Ohki, T., Hikage, T. & Watanabe, Y. (2010). *Chem. Eur. J.* **16**, 2730–2740.
Weierstall, U., Spence, J. C. H. & Doak, R. B. (2012). *Rev. Sci. Instrum.* **83**, 035108.
White, T. A., Kirian, R. A., Martin, A. V., Aquila, A., Nass, K., Barty, A. & Chapman, H. N. (2012). *J. Appl. Cryst.* **45**, 335–341.
Winn, M. D. *et al.* (2011). *Acta Cryst.* D**67**, 235–242.
Yabashi, M. & Tanaka, T. (2012). *Nature Photonics*, **6**, 648–649.
Zwart, P. H., Banumathi, S., Dauter, M. & Dauter, Z. (2004). *Acta Cryst.* D**60**, 1958–1963.